Running and Tumbling Localized Structures: A Non-Brownian Motion

F. R. Humire,[1] K. Alfaro-Bittner,[2] M. G. Clerc,[3] and R. G. Rojas[4]

[1]*Departamento de Física, Facultad de Ciencias, Universidad de Tarapacá, Casilla 7-D Arica, Chile*
[2]*Universidad Rey Juan Carlos, Calle Tulipán s/n, 28933 Móstoles, Madrid, Spain*
[3]*Departamento de Física and Millennium Institute for Research in Optics, FCFM, Universidad de Chile, Casilla 487-3, Santiago, Chile*
[4]*Instituto de Física, Pontificia Universidad Católica de Valparaíso, Casilla 4059, Valparaíso, Chile*

(Received 31 May 2024; accepted 2 October 2024; published 12 November 2024)

Macroscopic systems present particle-type solutions. Spontaneous symmetry-breaking can cause these solutions to travel in different directions, and the inclusion of random fluctuations can induce them to run and tumble. We investigate the running and tumbling of localized structures observed on a prototype model of one-dimensional pattern formation with noise. Statistically, the dynamics of localized structures are examined, particularly the mean square displacement as a function of time. It initially shows a diffusive behavior, replaced by a ballistic one, and finally manifests itself as diffusive again. We derive a minimal model for the position and velocity of localized structures, which reveals the origin of the observed dynamics.

DOI: 10.1103/PhysRevLett.133.207202

One of the most appealing phenomenon of macroscopic systems is the particlelike solutions [1–8]. The observed dynamical behaviors are characterized as being localized. Likewise, these behaviors are described by continuous parameters such as position and discrete parameters that take into account mobility, charge, and width, among other factors. The most paradigmatic and pioneering example is soliton or solitary waves observed when disturbing a water channel [5–7]. This type of solution has played a relevant role in modern telecommunications based on optical fibers [8]. During the last decades, a great effort has been put into the extension of this soliton concept from conservative to dissipative systems, in which these particlelike solutions are called dissipative localized structures (LS) [1–4]. Dissipative particlelike solutions have been observed in different fields, such as domains in magnetic materials, chiral bubbles in liquid crystals, current filaments in gas discharge, spots in chemical reactions and optical systems, localized states in driven fluid surface waves, oscillons in granular media, isolated states in thermal convection, and solitary waves in nonlinear optics, among others (see reviews [1–4] and references therein). For one-dimensional systems, the LS correspond to homoclinic curves in the corresponding associated spatial system [9]. The ingredients for observing these particlelike solutions are the coexistence of states and a characteristic length, which is achieved, for example, in systems that exhibit the coexistence of patterns and homogeneous states. A prototype model with these ingredients is the nonvariational Swift-Hohenberg equation, which has been proposed to describe the dynamics close to the confluence of nascent bistability and spatial instability, *Lifshitz point*, in various physical contexts such as nonlinear optics [10,11], chemical [11], elastic [12], acoustic [13], and biological systems [11]. This model equation exhibits a family of LS. As a result of the nonvariational terms, this solution can exhibit a spontaneous reflection symmetry-breaking and present a transition between motionless and traveling solutions (cf. Fig. 1) [14], which corresponds to a *nonequilibrium Ising-Bloch transition* [15–19]. Hence, depending on the initial condition, the LS can propagate towards one or the other flank. A similar phenomenon is observed in semiconductor lasers with absorbent saturable [20]. This phenomenon is the analog of domain propagation in magnetic systems [15], in which was introduced the nonequilibrium Ising-Bloch transitions, that is, the domain walls exhibit a spontaneous symmetry breaking and begin to propagate. This phenomenon has also been proposed and observed in liquid crystals [16], chemical reactions [17], optical [18] and mechanical systems [19]. Adding permanent fluctuations, noise can induce desymmetrization of the LS, causing them to propagate in one direction and abruptly tumble and propagate in the other direction (see Fig. 1). Running and tumbling is a phenomenon widely observed in the dynamics of bacteria [21,22], which exhibit a non-Brownian motion characterized by alternating ballistic and diffusive regime [23].

This Letter aims to study the running and tumbling of one-dimensional localized structures induced by random fluctuations. Based on a prototype model of localized structures with noise in the parameter that controls the transition between traveling and motionless localized structures, the run and tumble of LS is observed. The probability distribution of the LS position is characterized. The mean square displacement (MSD) is characterized as a function of time, we initially find a diffusive behavior,

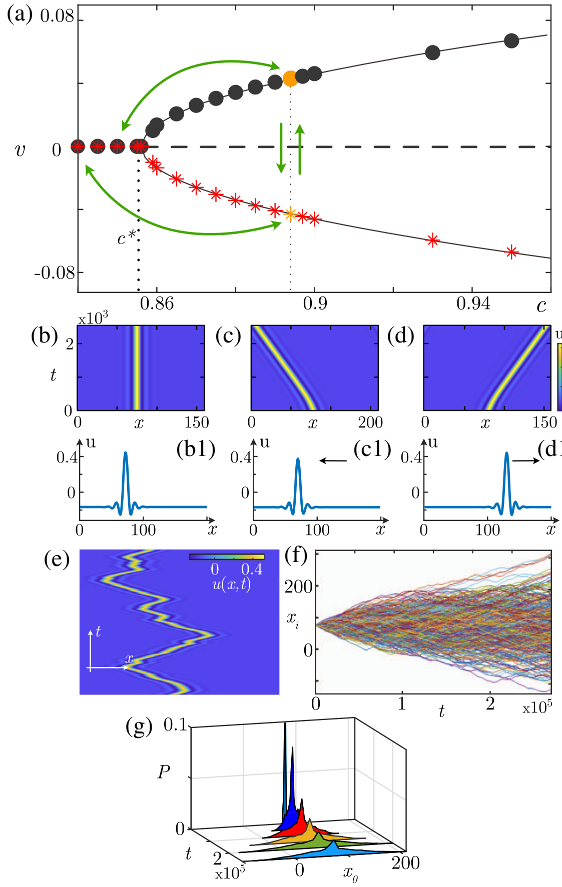

FIG. 1. Running and tumbling of LS of Eq. (1) with $\eta = -0.02$, $\mu = -0.092$, $\nu = 1.0$, $b = -1.0$, $a = 0$, $\Delta x = 0.8$, and $\Delta t = 0.03$. (a) Bifurcation diagram of the LS velocity as a function of parameter c. The transition between motionless and traveling solutions occurs at $c \equiv c^* = 0.856$ where the velocity has the form $v = \pm v_0\sqrt{c - c^*}$, $v_0 = 0.222$. The solid and dashed lines account for stable and unstable LS. The arrows show schematically noise-induced transitions between LS. (b),(c), and (d) The spatiotemporal evolution and profile of the static, traveling towards the left and right flank LS, respectively. (e) Spatiotemporal evolution of LS under the effect of random fluctuations with noise level intensity $a = 0.5$. (f) Temporal evolution of various LS trajectories from the same initial condition x_i. (g) Probability density distribution $P(x_0, t; x_i, t = 0)$ of LS position as a function of time.

which a ballistic one later replaces, and finally, a diffusive type is observed again. The observed behavior differs from the characteristic of bacterial movements due to the presence of an initial diffusive behavior. When the noise intensity level is changed, the typical behavior of the MSD remains the same. The coefficients that characterize these dynamics as a function of the noise intensity are revealed. By deriving a reduced model equation for the dynamics of the localized structure's position and velocity, we can obtain a bistable system for its velocity with noise. This minimal model allows us to analytically derive the evolution of the mean quadratic displacement. The minimal model is similar to those proposed to describe the dynamics of bacteria. However, it is a noise in the definition of speed, which is responsible for the diffusive regime for short times not reported in the context of bacterial dynamics. Numerical simulations of the model for semiconductor lasers with saturable absorbent qualitatively show the same behavior but only present the last regime for the MSD.

Prototype model of LS—As mentioned, essential elements for observing LS are the coexistence of equilibria and a characteristic length. These ingredients are naturally found around a Lifshitz point [24], characterized by the confluence of the nascent of bistability and spatial instability. Employing scale separation methods and normal form theory, this instability is described by (nonvariational Swift-Hohenberg equation) [10–13],

$$\partial_t u = \eta + \mu u - u^3 - \nu\partial_x^2 u - \partial_x^4 u + 2bu\partial_x^2 u + [c + \sqrt{a}\xi(x,t)](\partial_x u)^2, \tag{1}$$

where $u(x,t)$ is a scalar order parameter that can account for light intensity, chemical concentrations, average molecular orientations, radial displacement, among others. μ is the bifurcation parameter. η parameter controls the bistable region. ν is the diffusion (< 0) or antidiffusion (> 0) coefficient. b and c stand for the nonlinear diffusion and advection, respectively. $\xi(x,t)$ is a Gaussian white noise with zero mean value $\langle\xi(x,t)\rangle = 0$, $\langle\cdot\rangle$ is the average overall noise realizations, correlation $\langle\xi(x,t)\xi(x',t')\rangle = \delta(t-t')\delta(x-x')$, i.e., the noise has not temporal and spatial memory, and a represents the noise level intensity.

Running and tumbling LS—Numerical simulations of model Eq. (1) show LS, which present a transition between motionless and traveling LS, nonequilibrium Ising-Bloch transitions, when increasing the nonvariational parameter c associated with nonlinear advection [14]. Figure 1 shows the typical localized structures of model Eq. (1) and its respective bifurcation diagram for its velocity as a function of parameter c. By including the effects of fluctuations of the nonlinear advection parameter c in the region of localized propagative structures, we numerically observe the running and tumbling of localized structures. In all numerical simulations, we consider as an initial condition a localized state that corresponds to a motionless LS obtained with $c < c^*$. Figure 1(e) illustrates the typical spatiotemporal dynamics observed for localized structures. In order to figure out the statistical dynamics of LSs, we consider many realizations that start with the same initial condition, $x = x_i$, depicted in Fig. 1(f). From these trajectories, we can calculate the probability distribution density of the position $P(x_0, t; x_i, t = 0)$ of the localized structures for each instant of time, where x_0 accounts for the position of LS at time t. Figure 1(g) summarizes the results found for the evolution of the position probability distribution density. From this chart, we conclude that the localized structures present a

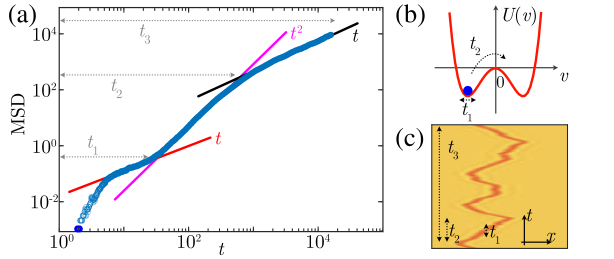

FIG. 2. Statistical analysis of random displacement of the localized structures of model Eq. (1) with $\eta = -0.02$, $\mu = -0.092$, $\nu = 1$, $b = -1.0$, $c = 0.865$, $a = 0.5$, $\Delta x = 0.8$, $\Delta t = 0.03$. (a) Mean square displacement of the LS as a function of time. The straight lines and their respective exponents account for the different regimes. t_1, t_2, and t_3 are characteristic times that account for the diffusive, ballistic, and diffusive regimes, respectively. (b) Bistable potential $U(v)$ for the LS velocity, which qualitatively describes the running and tumbling dynamics. (c) Spatiotemporal dynamics of run and tumble of LS and their time characteristics.

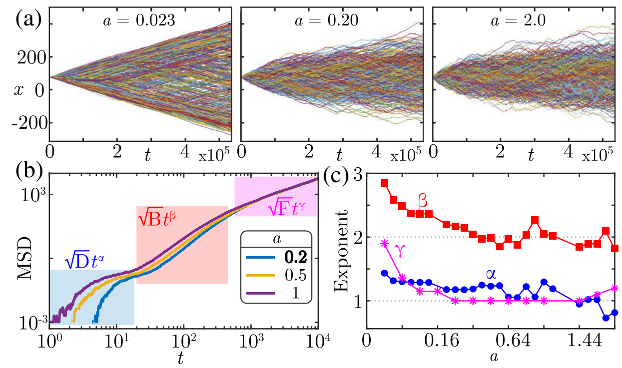

FIG. 3. Characterization of the dispersion of localized structures of model Eq. (1) by $\eta = -0.02$, $\mu = -0.092$, $\nu = 1$, $b = -1.0$, $c = 0.865$, $\Delta x = 0.8$, $\Delta t = 0.03$. (a) Spatiotemporal trajectories of the LSs for different noise level intensity. The different colors show the different trajectories. (b) MSD for different noise levels $a = 0.2$, $a = 0.5$, and $a = 1.0$. (c) Exponents of the MSD(t) as a function of noise intensity level a.

dispersive process. To characterize this dispersive process, we have calculated the mean square displacement MSD $= \langle (x_0 - \langle x_0 \rangle)^2 \rangle$. Figure 2(a) summarizes the temporal evolution of the MSD. From this chart, we initially observe a transient that immediately follows a power law t ($t \leq t_1$ in Fig. 2), which means that the LS presents a diffusive behavior later this behavior is replaced by a power law t^2 ($t_1 \leq t \leq t_2$ in Fig. 2), which accounts for a ballistic behavior and finally the system again presents a power law t ($t > t_3$ in Fig. 2), diffusive behavior, for long times. The observed dynamics can be understood qualitatively as a bistable potential $U(v)$ for velocity with noise when the system is initiated from the unstable point, [see Fig. 2(b)]. In fact, when the LS moves in one direction for a short time, it exhibits small oscillations to speed. These dynamics are represented as fluctuations around the minimum power [see Figs. 2(b) and 2(c)]. For a long enough time, fluctuations can induce a transition between the minima ($t \sim t_2$), causing the LS to tumble and propagate in the other direction. Note that t_2 is characterized by the mean first passage time [25]. For times larger than the mean first passage time, the LS fluctuates without sensing the presence of the bistable potential structure.

To study the universality of the curve found for MSD, we have carried out a large number of numerical simulations for different values of the noise intensity level a. Figure 3(a) depicts the type of trajectories found for various noise levels. Likewise, we have determined the MSD for different noise levels, see Fig. 3(b). We note that qualitatively the observed curves are similar and all present the same regimes. The shift of the small MSD curve is due to the fact that the small MSD value is reached more quickly at higher noise levels. To characterize the different regions we can approximate the MSD by region

$$\mathrm{MSD}(t) = \begin{cases} \sqrt{D}t^{\alpha}, & t \leq t_1, \\ \sqrt{B}t^{\beta}, & t_1 \leq t \leq t_2, \\ \sqrt{F}t^{\gamma}, & t \geq t_2. \end{cases} \tag{2}$$

Figure 3(c) shows the different exponents $\{\alpha, \beta, \gamma\}$ as a function of noise intensity level a. This graph shows that the tendency of the exponents is to decrease as a function of the noise level. Notice that the running and tumbling observed in bacteria only exhibit the last two regimes [23], that is, ballistic and diffusive regimes.

In brief, the dynamics of traveling localized structures exhibit a non-Brownian motion characterized by alternating from a diffusive ballistic to a diffusive regime. When considering Eq. (1) with homogeneous noise, $\xi = \xi(x, t)$, the running-and-tumble phenomenon does not take place since the noise cannot spatially dissymmetry the LS and then change its propagation direction and flip it. Hence, we expect the phenomenon to be observed for uncorrelated or finitely correlated spatiotemporal noises.

Particle-type description of LS—To describe the dynamics of the LS, i.e., the position and velocity, we consider the strategy used in Ref. [14], in which the system is studied close to the transition of travel to motionless LSs, where $c = c^* + \epsilon c_0$ with $\epsilon \ll 1$ (cf. Fig. 1). Let us consider the ansatz $u(x, t) = u_{sl}[x - x_0(\epsilon t)] + \epsilon v_0(\epsilon^2 t) u_{as}[x - x_0(\epsilon t)] + w(x, x_0, v_0)$, where u_{sl} and u_{as} are the symmetrical and asymmetrical part of the LS. x_0 and v_0 are the positions and the amplitudes of the asymmetrical part of the LS. Note that temporal scales of x_0 and v_0 are different [14]. Introducing the above ansatz in model Eq. (1), linearized in w and imposing the solvability condition, after straightforward calculations, we get the dominant order (the particle-type equation, the reduced model)

$$\frac{dv_0}{dt} = \sigma v_0 - v_0^3 + \eta_1(t) = -\frac{\partial U(v_0)}{\partial v_0} + \eta_1(t),$$
$$\frac{dx_0}{dt} = v_0 + \eta_2(t), \tag{3}$$

with the bifurcation parameter $\sigma \equiv 2\epsilon c_0 \langle\langle \psi_1 | \partial_x u_{as} \partial_x u_{ls} \rangle\rangle / \langle\langle \psi_1 | u_{as} \rangle\rangle$ that is proportional to $c - c^*$. The stochastic terms $\eta_1(t) = a\langle\langle \psi_1 | \xi(x,t)(\partial_x u_{ls})^2 \rangle\rangle / \langle\langle \psi_1 | u_{as} \rangle\rangle$ and $\eta_2(t) = -a\langle\langle \psi_0 | \xi(x,t)(\partial_x u_{ls})^2 \rangle\rangle / \langle\langle \psi_0 | \partial_x u_{ls} \rangle\rangle$ account for the Gaussian white noise without memory, i.e., $\langle \eta_1(t) \rangle = \langle \eta_2(t) \rangle = 0$, $\langle \eta_1(t)\eta_1(t') \rangle = a_1 \delta(t-t')$, and $\langle \eta_2(t)\eta_2(t') \rangle = a_2 \delta(t-t')$. ψ_0 and ψ_1 are critical modes of linear adjoint operator [14], and the symbol $\langle\langle f|g \rangle\rangle \equiv \int fg dx$ stands for the inner product. Hence, the dynamics of localized structures are characterized by having a Langevin equation for velocity v_0 with a symmetric bistable potential $U(v_0) = -\sigma v_0^2/2 + v_0^4/4$ with minima at $\pm\sqrt{\sigma}$. The bistable potential for the velocity v_0 is illustrated in Fig. 2(b). Note that a Langevin equation relates the position and velocity of the LS; that is, speed and position are not simply related by definition. Namely, a Langevin equation with inertia does not describe the set of Eqs. (3). From model Eq. (3) and the noise-induced transition phenomenon, one expects that the trajectories present a running and tumbling behavior.

The reduced dynamical model (3) from the resting configuration $v_0(t=0) = 0$ is initially characterized because the LS is initially characterized because the LS acquires a speed towards a flank (minimum of the potential) and begins to fluctuate around that speed ($t \leq t_2$ in Fig. 2). Subsequently, for times on the order of the mean first passage time, the LS can stop and change the direction of propagation ($t \geq t_2$ in Fig. 2) and again perform this dynamic cycle (running and tumbling), as illustrated in Fig. 2(c). Therefore, the reduced model Eq. (3) adequately captured the dynamics of the localized structures of the nonvariational Swift-Hohenberg Eq. (1). Neglecting the cubic term of the reduced model (3), one can describe the dynamics around the unstable and stable equilibrium point, where only the linear constant σ is changed to -2σ. we can perform a similar calculation to obtain the MSD that carried out by Chandrasekhar [26]; after straightforward calculations, we get

$$\begin{aligned}\mathrm{MSD} = {} & \left(\frac{(A_0 + \sqrt{\sigma})}{2\sigma}(e^{-2\sigma t} - 1)\right)^2 \\ & + \frac{a_1}{8\sigma^3}[4\sigma(a_1 - 2\sigma a_2/\sqrt{a_1})^2 t - 3a_1^2 + 8a_1 a_2 \sigma \\ & + 4a_1(a_1 - 2\sigma a_2)e^{-2\sigma t} - a_1^2 e^{-4\sigma t}],\end{aligned} \tag{4}$$

where $A_0 \equiv v_0(t=0)$ is the initial speed. Formula (4) is linear in time for short times; then, it is corrected with quadratic terms when the time increases, and finally, for a very long time, it is linear again. Hence, it is in agreement with the MSD expression (2) and numerical simulations of models (1) and (3). Figure 4(a) shows the MSD obtained from simulating the reduced Eq. (3) and their typical temporal trajectories for different noise intensity levels agree with formula (4).

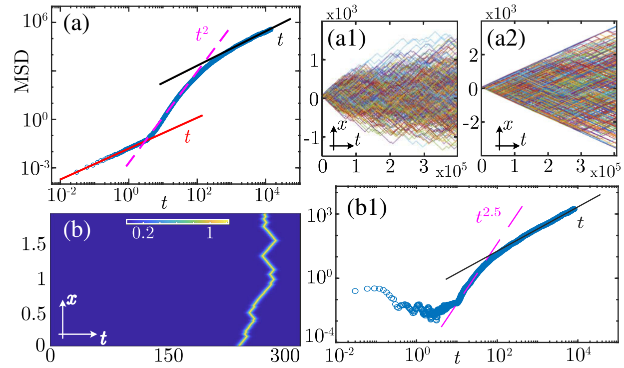

FIG. 4. Running and tumbling of LSs. (a) MSD obtained from numerical simulation of the reduced model Eq. (3) by $\sigma = 0.1$, $a_1 = 0.12$, and $a_2 = 0.24$. Panels (a1) and (a2) show temporal trajectories for different intensity levels of noise of a_1, $a_1 = 0.12$, and $a_1 = 0.031$, respectively. (b) Spatiotemporal trajectory of the amplitude $|\psi|$ of the LS obtained by numerical simulation of the stochastic amplitude Eq. (5) by $\mu = -0.05$, $\beta_r = 1.22$, $\beta_i = 0.7$, $\gamma_r = -1.0$, $\gamma_i = 0.5$, $a = 0.003$, $\Delta x = 0.5$, and $\Delta t = 0.05$. Panel (b1) MSD obtained from numerical simulation of the stochastic amplitude Eq. (5) with the same parameter. The segmented ($t^{2.5}$) and solid line (t) show the trend observed in the different running and tumbling regimes of the LSs.

Transitions from motionless to moving LS have also been observed in optical [27,28] and gas discharge experiments [2]. To shed light the universality of this phenomenon, let us consider the cubic-quintic Ginzburg-Landau equation with diffraction, in which a transition from propagative to motionless pulses has recently been reported [20], the amplitude equation reads

$$\frac{\partial \psi}{\partial t} = [\mu + \sqrt{a}\xi(x,t) + \beta|\psi|^2 + \gamma|\psi|^4]\psi + i\frac{\partial^2 \psi}{\partial x^2}, \tag{5}$$

where $\psi(x,t)$ is a complex order parameter, μ is the bifurcation parameter, the complex coefficient $\beta = \beta_r + i\beta_i$ and $\gamma = \gamma_r + i\gamma_i$ account for nonlinear dissipation and saturation (real parts) and phase response (imaginary parts). $\xi(x,t) = \xi_r(x,t) + i\xi_i(x,t)$ is a complex Gaussian white noise with mean value $\langle \xi(x,t) \rangle = 0$ and correlation $\langle \xi(x,t)\bar{\xi}(x',t') \rangle = 2\delta(t-t')\delta(x-x')$. Note that the previous model Eq. (5) was derived for a semiconductor laser with absorber saturable medium [20], where ψ accounts for electric field envelope and μ is proportional to the critical pumping.

Numerical simulations of the stochastic amplitude Eq. (5) show the running and tumbling of localized structures. Figure 4(b) illustrates a typical trajectory of a localized structure with running and tumbling, obtained through numerical simulations of the stochastic amplitude

Eq. (5). To characterize the statistical dynamics of these localized structures with running and tumbling, we have calculated the MSD of trajectories. Figure 4(b1) summarizes the results found, where we identified three regimes: transient phase and amplitude adaptation, superballistic with MSD $\sim t^{2.5}$, and diffusive behavior with MSD $\sim t$. Characterization of the role of phase amplitude in the observed dynamics is in progress.

In conclusion, particlelike solutions of one-dimensional field equations that present a transition between traveling and motionless solutions under the influence of inherent fluctuations present running and tumbling. This non-Brownian dynamic is statistically characterized by presenting a mean square displacement as a function of time. Initially, the displacement shows a diffusive behavior, which a ballistic one then replaces. Finally, the displacement manifests itself again as diffusive. Transitions from motionless to traveling LS have also been observed in one-dimensional optical systems [27,28], and two dimensions optical [29] and gas discharge experiments [2]; the study of running and tumbling of two-dimensional localized structures is in progress. Model Eq. (1) describes an optical valve with optical feedback [10]; this is a flexible experiment where the running and tumbling of LS can be studied in a quasi-one-dimensional configuration.

Acknowledgments—F. R. H. acknowledges support from the Dirección General de Investigación e Innovación de la Universidad de Tarapacá, Arica, Chile, under the Proyecto UTA Mayor No. 4735-24. M. G. C. acknowledges the financial support of ANID-Millennium Science Initiative Program-ICN17_012 (MIRO) and FONDECYT Project No. 1210353.

[1] *Localized States in Physics: Solitons and Patterns*, edited by O. Descalzi, M. Clerc, S. Residori, and G. Assanto (Springer, New York, 2010).

[2] H. G. Purwins, H. U. Bödeker, and Sh. Amiranashvili, Dissipative solitons, Adv. Phys. **59**, 485 (2010).

[3] *Dissipative Solitons: From Optics to Biology and Medicine*, Lecture Notes in Physics Vol. 751, edited by N. Akhmediev and A. Ankiewicz (Springer, Heidelberg, 2008).

[4] E. Knobloch, Spatial localization in dissipative systems, Annu. Rev. Condens. Matter Phys. **6**, 325 (2015).

[5] J. Scott Russell, Report on waves, *Report of the 14th meeting of the British Association for the Advancement of Science, Plates XLVII-LVII* (Jonh Murray, London, 1845), pp. 311–390.

[6] A. C. Newell, *Solitons in Mathematics and Physics* (Society for Industrial and Applied Mathematics, Philadelphia, 1985).

[7] M. Remoissenet, *Waves Called Solitons: Concepts and Experiments* (Springer Science & Business Media, Heidelberg, 2013).

[8] J. R. Taylor, *Optical Solitons: Theory and Experiment* (Cambridge University Press, Cambridge, England, 1992).

[9] P. Coullet, Localized patterns and fronts in nonequilibrium systems, Int. J. Bifurcations Chaos, **12**, 2445 (2002).

[10] M. G. Clerc, A. Petrossian, and S. Residori, Bouncing localized structures in a liquid-crystal-light-valve experiment, Phys. Rev. E **71**, 015205(R) (2005).

[11] G. Kozyreff and M. Tlidi, Nonvariational real Swift-Hohenberg equation for biological, chemical, and optical systems, Chaos **17**, 037103 (2007).

[12] N. Stoop, R. Lagrange, D. Terwagne, P. M. Reis, and J. Dunkel, Curvature-induced symmetry breaking determines elastic surface patterns, Nat. Mater. **14**, 337 (2015).

[13] L. Perez-Arjona, V. J. Sanchez-Morcillo, and G. J. de Valcarcel, Ultrasonic cavity solitons, Europhys. Lett. **82**, 10002 (2008).

[14] A. J. Alvarez-Socorro, M. G. Clerc, and M. Tlidi, Spontaneous motion of localized structures induced by parity symmetry breaking transition, Chaos **28**, 053119 (2018).

[15] P. Coullet, J. Lega, B. Houchmandzadeh, and J. Lajzerowicz, Breaking chirality in nonequilibrium systems, Phys. Rev. Lett. **65**, 1352 (1990).

[16] J. M. Gilli, M. Morabito, and T. Frisch, Ising-Bloch transition in a nematic liquid crystal, J. Phys. II (France) **4**, 314 (1994).

[17] D. Haim, G. Li, Q. Ouyang, W. D. McCormick, H. L. Swinney, A. Hagberg, and E. Meron, Breathing spots in a reaction-diffusion system, Phys. Rev. Lett. **77**, 190 (1996).

[18] D. Michaelis, U. Peschel, F. Lederer, D. V. Skryabin, and W. J. Firth, Universal criterion and amplitude equation for a nonequilibrium Ising-Bloch transition, Phys. Rev. E **63**, 066602 (2001).

[19] M. G. Clerc, S. Coulibaly, and D. Laroze, Non-variational Ising-Bloch transition in parametrically driven systems, Int. J. Bifurcation Chaos Appl. Sci. Eng. **19**, 2717 (2009).

[20] F. R. Humire, K. Alfaro-Bittner, M. G. Clerc, and R. G. Rojas, Transition from traveling to motionless pulses in semiconductor lasers with saturable absorber, Physica (Amsterdam) **458D**, 133994 (2024).

[21] W. R. DiLuzio, L. Turner, M. Mayer, P. Garstecki, D. B. Weibel, H. C. Berg, and G. M. Whitesides, Escherichia coli swim on the right-hand side, Nature (London) **435**, 1271 (2005).

[22] M. Jaan, R. Driessen, P. Galajda, J. E. Keymer, and Cees Dekker, Bacterial growth and motility in sub-micron constrictions, Proc. Natl. Acad. Sci. U.S.A. **106**, 14861 (2009).

[23] X. L. Wu and A. Libchaber, Particle diffusion in a quasi-two-dimensional bacterial bath, Phys. Rev. Lett. **84**, 3017 (2000).

[24] R. M. Hornreich, L. Marshall, and S. Shmuel, Critical behavior at the onset of k space instability on the lambda line, Phys. Rev. Lett. **35**, 1678 (1975).

[25] N. G. Van Kampen, *Stochastic Processes in Physics and Chemistry*, (Elsevier, Amsterdam, 1992).

[26] S. Chandrasekhar, Stochastic problems in physics and astronomy, Rev. Mod. Phys. **15**, 1 (1943).

[27] L. Spinelli, G. Tissoni, L. A. Lugiato, and M. Brambilla, Thermal effects and transverse structures in semiconductor

microcavities with population inversion, Phys. Rev. A **66**, 023817 (2002).

[28] P. V. Paulau, D. Gomila, P. Colet, M. A. Matias, N. A. Loiko, and W. J. Firth, Drifting instabilities of cavity solitons in vertical-cavity surface-emitting lasers with frequency-selective feedback, Phys. Rev. A **80**, 023808 (2009).

[29] A. J. Scroggie, J. M. McSloy, and W. J. Firth, Self-propelled cavity solitons in semiconductor microcavities, Phys. Rev. E **66**, 036607 (2002).